Influence of the Blood Glucose Concentration on FDG Uptake in Cancer—A PET Study

Paula Lindholm, Heikki Minn, Sirkku Leskinen-Kallio, Jörgen Bergman, Ulla Ruotsalainen and Heikki Joensuu

Department of Oncology and Radiotherapy, Department of Nuclear Medicine, Turku University Central Hospital, Turku Medical Cyclotron-PET Center, Radiochemistry Laboratory, Turku University, Turku, Finland

Radiolabeled [^{18}F]-2-fluoro-2-deoxy-D-glucose (FDG) is a glucose analogue widely used to study tumor metabolism by means of positron emission tomography (PET). Little is known about the effect of hyperglycemia on FDG uptake and PET imaging of tumors. Five patients with head and neck cancer underwent two PET studies prior to cancer therapy, first in the fasting state and then 2–5 days later after oral glucose loading. FDG uptake was measured with standardized uptake values (SUV) and K_i values according to Patlak et al. The fasting SUVs ranged from 4.1 to 10.9 and K_is from 0.021 min^{-1} to 0.067 min^{-1}, whereas after loading both the SUVs (range 2.2–5.9, $p < 0.02$) and K_i values (range 0.006–0.042 min^{-1}, $p < 0.05$) decreased significantly, and the quality of the PET images became markedly poorer. The FDG metabolic rate ($K_i \times$ P-Gluc) remained similar in different plasma glucose concentrations in tumors, but increased clearly in muscles after loading. Therefore, patients entering PET-FDG studies should fast and their blood glucose concentration needs to be taken into account when evaluating FDG accumulation.

J Nucl Med 1993;34:1–6

Glucose utilization in malignant tissues tends to be high (*1–3*). This is clearly seen in rapidly growing, poorly differentiated tumors (*4*). Elevated glucose utilization depends on the increased rate of glucose transport through the cell membrane, the decreased rate of dephosphorylation and the enhanced activity of the key glycolytic enzymes, e.g., hexokinase (*5*). Altered glucose metabolism can be studied with radiolabeled glucose analogues such as [^{18}F]-2-fluoro-2-deoxy-D-glucose (FDG) (*6–8*). FDG is rapidly transported into tumor cells and phosphorylated by hexokinase. Since FDG is not catabolized further, it remains metabolically trapped intracellularly as FDG-6-phosphate. FDG accumulation in tumor cells can be measured noninvasively in vivo by means of positron emission tomography (PET) (*9–10*).

Received Apr. 10, 1992; revision accepted Jul. 17, 1992.
For correspondence or reprints contact: Paula Lindholm, MD, Department of Oncology and Radiotherapy, Turku University Central Hospital, SF-20520 Turku, Finland.

FDG uptake rate in cardiac and skeletal muscles is enhanced by high plasma glucose levels (*11*). In vitro studies indicate that FDG accumulation in cancer cells will decline with increasing glucose level in the medium (*12*). A decrease of the mean FDG uptake has been observed at very high blood glucose and insulin levels in tumors of rodents (*13*).

FDG is a useful tumor-detecting agent for different kinds of human cancer (*14,15*), but there have been only a few human studies on the influence of elevated blood glucose level on FDG uptake in tumors (*16*). This is of considerable importance if FDG accumulation is to be correlated with the malignant potential of cancer (*17–21*). The purpose of this investigation was to evaluate whether hyperglycemia alters tumor FDG uptake or changes the quality of PET images. FDG uptake of head and neck tumors was evaluated before cancer treatment both when the patient was in the fasting state and after oral glucose loading.

PATIENTS AND METHODS

Patients

Five patients with head and neck cancer were entered into the study after written informed consent was obtained. None of the patients was known to have abnormal glucose tolerance or diabetes. The patients were not cachectic; the body mass index (BMI) (*22*) calculated as

$$\text{BMI} = \frac{\text{weight (kg)}}{(\text{height})^2\ (\text{m}^2)} \qquad \text{Eq. 1}$$

varied between 20.5 and 27.8 (mean 24.4).

All tumors were histologically primary squamous cell carcinomas (SCC) of the head and neck region. Clinical staging included endoscopic examination, ultrasonography and computed tomography (CT) when feasible. Staging of the tumors was performed according to the UICC TNM classification of malignant tumors (*23*). Patient characteristics are described in Table 1.

The study was approved by the Ethical Committee of Turku University Central Hospital.

PET Imaging and Methods

FDG was synthesized by a method modified from the synthesis of Hamacher et al. (*24*). The radiochemical purity of FDG was

TABLE 1
Patient Characteristics

Patient no.	Age	Sex	BMI	Site of tumor	Tumor size (mm)	Stage by UICC†	Grade‡
1	71	F	23.6	Tongue, SCC	28×20	$T_2N_0M_0$	1
2	50	M	27.8	Tongue, SCC	25×35	$T_2N_0M_0$	1
3	62	M	20.4	Hypopharynx, SCC	60×30	$T_3N_1M_0$	2
				Neck metastasis	10×10		
4	75	M	23.8	Lower lip, SCC	45×25	$T_3N_2M_0$	2
				Neck metastasis, left	30×30		
				Neck metastasis, right	15×10		
5	63	M	26.5	Larynx, SCC	22×20	$T_2N_2M_0$	2
Mean			24.4	Neck metastasis	40×30		

‡ Histological grade 1 and 2, well and moderately differentiated, respectively.
BMI = body mass index (22), SCC = squamous cell carcinoma and †UICC = International Union Against Cancer (23).

99.0% ± 0.4% and the specific activity about 2 Ci/μmol at the end of the synthesis.

The first PET-FDG study was performed in the fasting state. After fasting overnight, the patients underwent transmission scanning for attenuation correction. The transmission scanning was performed with a removable ^{68}Ge ring source. After transmission scanning, FDG (270–300 MBq) was injected into a peripheral vein of the arm and dynamic emission scanning was carried out for 60 min (4 × 30 sec scans, 3 × 60 sec, 5 × 180 sec, 8 × 300 sec).

Another PET study with glucose loading for each patient was performed within 2–5 days after the fasting study. The patients received no treatment nor had a biopsy between the two PET studies. One hour prior to the FDG injection, the patient drank 200 ml of glucose solution (Glucodyne®, Medica, Oulu, Finland) containing 50 g of glucose (Patient 3 received 70 g, Table 2). Plasma glucose and insulin levels were measured immediately before the glucose load (baseline samples) and then every 30 min. One hour after glucose loading, FDG was injected and PET scanning was performed for 60 min.

Using a heating pad to warm the arm, frequent venous samples for measurements of the plasma radioactivity concentration were taken from an antecubital vein of the arm opposite to the injection site. The measured plasma glucose and insulin values are shown in Table 2. All fasting plasma insulin values were normal, but Patients 1 and 5 had an abnormal glucose tolerance (Table 2).

The PET scanning device was an ECAT scanner type 931/08–12, which produces 15 contiguous slices with a slice thickness of 6.7 mm and an axial resolution of 6.1 mm full width at half maximum in the center of the field of view.

Several regions of interest (ROIs) were drawn on the hot spots of tumorous and normal tissues. The size of the ROIs ranged from 12 to 41 pixels and the relative standard deviation of the measured average radioactivity in the ROI was less than 14% in the last frame. When studying the uptake of normal tissue, the ROIs in Patients 1 and 2 were drawn on the hot spots of the cerebellum, because in contrast to muscles, the cerebellum was visible both in fast and load. When studying the uptake of normal tissue in the other patients, FDG uptake in the tongue or the cervical muscles was measured. The emission images generated during the fasting state and after glucose loading were compared with the respective transmission images in order to make sure that the corresponding planes in the two PET studies were analyzed.

FDG accumulation was measured using the standardized up-

TABLE 2
Plasma Glucose and Insulin Values in the Fasting State and After Glucose Loading in Five Patients with Head and Neck Cancer

Patient no.		Plasma Glucose (mmol/liter)						Plasma Insulin (mU/liter)				
		−60 min	−30 min	0 min†	+30 min	+60 min	Mean*	−60 min	−30 min	+0 min†	+30 min	+60 min
1	Fast			5.4	5.2	5.3	5.3			3		
	Load	5.5	8.0	8.6	12.2	10.5	10.4	6	47	47	43	37
2	Fast			4.7	5.7	5.9	5.4			8		
	Load	5.8	7.7	7.9	8.3	7.8	8.0	11	58	76	42	50
3	Fast			6.6	5.8	5.3	5.9			8		
	Load	7.0	7.9	13.1	13.8	10.2	12.4	6	17	54	67	55
4	Fast			4.8	4.9	5.1	4.9			10		
	Load	5.2	6.4	9.3	9.9	6.8	8.7	10	40	67	84	36
5	Fast			5.4	5.5	5.8	5.6			4		
	Load	6.4	9.5	10.2	10.4	10.2	10.3	7	43	39	44	50

* Mean × the average plasma glucose level during scanning.
† Plasma glucose and insulin values immediately before FDG injection.

take value (SUV) as follows:

$$SUV = \frac{\text{radioactivity concentration in ROI [Bq cm}^{-3}\text{]}}{\text{injected dose [Bq]/weight of the patient (g)}}. \quad \text{Eq. 2}$$

Radioactivity concentration in the ROI was determined as the maximum average radioactivity concentration in the tissue at 55 to 60 min postinjection, corrected for calibration and decay. FDG uptake rate from plasma to tumor was calculated as K_i values according to Patlak et al. (*25*). The last 11 data points representing the time between 11 and 60 min postinjection were used to produce the influx curve. FDG metabolic rate (MR_{FDG}) was assessed by multiplying K_i values by the average plasma glucose value during the emission scanning as follows:

$$MR_{FDG} = \frac{1}{LC} \times K_i \times \text{P-Gluc (mean)}\ \mu\text{mol/100g/min}, \quad \text{Eq. 3}$$

where the lumped constant (LC) (*26*) was assumed to be one. The metabolic index of FDG was calculated similarly by multiplying the SUVs by the average plasma glucose values.

The SUVs and K_i values were compared with each other by linear regression and the Pearson correlation coefficient (r) was calculated. Wilcoxon signed-rank test was used to compare FDG uptake in the fast and load studies.

RESULTS

All primary tumors were visualized clearly in the studies performed in the fasting state. Although the tongue cancer in Patient 2 could not be detected by CT, the tumor was visible with PET imaging. In contrast, a small palpable neck metastasis located near the right angle of the mandible that was visible in ultrasonography and was verified by fine needle biopsy could not be detected with PET-FDG probably because of resolution limits (Patient 4).

The fasting SUVs of tumors ranged from 4.1 to 10.9 (Table 3). After loading, the SUVs decreased significantly, ranging from 2.2 to 5.9 ($p < 0.02$), some even more than 50%, as shown in Figure 1. The uptake rate of FDG in the cerebellum also became lower after loading. In contrast to the tumors and the cerebellum, the tongue and the neck muscles accumulated more FDG after loading, resulting in blurring of the tumor margins and less clear localization of tumors. Consequently, glucose loading remarkably impaired the quality of PET images (Fig. 2).

The fasting K_i values of tumors ranged from 0.021 min^{-1} to 0.067 min^{-1} (Table 4). After loading, the K_is decreased markedly (range 0.006–0.042 min^{-1}, $p < 0.05$) except in Patient 4, in whom the K_i value of the lip tumor remained about the same and the K_i value of the neck metastasis was higher than that under the fasting conditions (Patient 4 was also included in statistical analysis). The linearity of the Patlak plots was good in all studies (r^2 0.84–0.98, mean 0.91) except in one study performed in the fasting state (Patient 4, $r^2 = 0.71$). The correlation between the SUVs and the K_is was excellent ($r = 0.87$, $p < 0.0001$, fast and load studies combined).

The metabolic index of tumor FDG (SUV × P-Gluk) remained quite stable when calculated in the fasting state and after glucose loading (Table 3). The index was on average only 10% higher after loading, while MR_{FDG} (K_i × P-Gluk) was on average 36% higher after loading when compared with the fasting state (Table 4). This is because in one case (Patient 4) the K_is did not decrease after glucose loading. However, in muscle tissue the product SUV × P-Gluc increased more than twofold (Table 3) and K_i × P-Gluc almost fivefold (Table 4). Hence, the visual delineation of the tumor became generally less clear in images generated during glucose loading.

DISCUSSION

After loading, a decrease in the SUVs was found in all tumors studied. In contrast to the tumors, the muscle

TABLE 3
FDG Uptake Calculated Using the Standardized Uptake Value (SUV)

Patient no.	Tumor/organ, body part	SUV		% Load	P-Gluc × SUV		% Load
		Fast	Load	Fast	Fast	Load	Fast
1	Primary	9.2	3.8	42	48.7	39.8	82
2	Primary	6.9	5.9	85	37.2	46.8	126
3	Primary	10.9	4.8	43	64.5	58.9	91
	Metastasis	4.1	2.2	54	24.2	27.4	113
4	Primary	7.9	4.2	53	38.9	36.6	94
	Metastasis	4.6	4.2	91	22.4	36.3	162
5	Primary	5.6	3.3	58	31.5	33.6	107
	Metastasis	6.3	3.7	58	35.3	37.8	107
	Mean	6.9	4.0	60.5	37.8	39.7	110
1		10.0	3.6	36	52.7	37.2	71
2		8.8	5.3	60	47.6	42.2	89
3	Tongue	2.7	3.5	127	16.2	43.3	267
4	Tongue	3.9	4.2	107	19.0	36.1	190
5	Tongue	2.8	2.8	101	15.7	29.3	187
	Muscle (neck)	2.5	3.1	125	13.8	31.8	230
	Mean	3.0	4.0	115	16.2	31.5	219

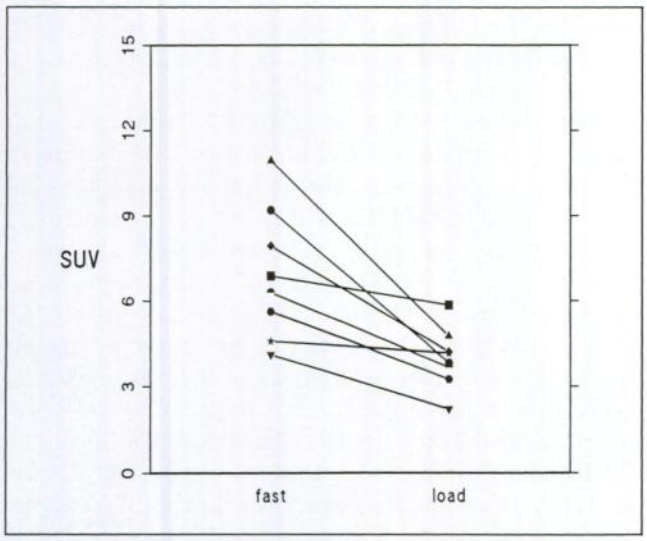

FIGURE 1. Standardized uptake values (SUVs) of eight malignant head and neck tumors (five primary tumors and three neck metastases) in the fasting state and after oral glucose loading.

tissue accumulated somewhat more FDG after loading than in the fasting state, which resulted in blurring of the tumor margins. Similarly, all except one of the tumors studied had a smaller K_i value after loading.

FDG uptake in cancer is sensitive to variations in the blood glucose concentration. PET-FDG studies may be particularly unreliable in diabetic patients. The blood glucose concentration should be always considered when grading or staging tumors or trying to correlate a change in the FDG uptake with a treatment response. However, in this series of five patients, the product $K_i \times$ P-Gluc and SUV $\times$ P-Gluc seemed to remain quite stable in tumors after loading. This may suggest that the product $K_i \times$ P-Gluc or SUV $\times$ P-Gluc could be used for correction of FDG uptake if PET-FDG studies need to be repeated at different blood glucose levels.

After loading, the metabolic rate for FDG increased about fivefold and the metabolic index about twofold in muscles. Apparently, when plenty of glucose is available to cells, its use is increased in muscles, resulting in a greater influx of FDG. In contrast, glucose utilization in most cancers does not appear to depend on the plasma glucose concentration. Hence, relatively more FDG as compared with unlabeled glucose is taken up by the cancer cells when the extracellular glucose concentration is low, resulting in higher SUVs and K_is in the fasting state. However, there may be exceptions to this rule (e.g., the lip cancer of Patient 4).

In addition to hyperglycemia, oral glucose loading resulted in rapidly increasing plasma insulin concentrations. The influence of hyperinsulinaemia on FDG uptake is not known in human tumors. However, oral glucose loading results in variable and unstable metabolic conditions (*11*). Consequently, the effect of elevated plasma insulin level on tumor FDG uptake could not be estimated in this study.

Glycolytic enzyme activity in tumorous tissue is heterogeneous (*27*), and glucose metabolic rates vary largely (*28, 29*). An association with tumor grade may depend on the type of the tumor. The LC value for head and neck cancer is not known. Different tumors may possess different kinds of LCs, and, moreover, the tumor itself may contain parts with different values for the LC (*30, ,31*). In this study, the LC for tumor is assumed to be 1.0. This might be acceptable, but we do not suggest that the LC for head and neck cancer is always a fixed value such as 1.0; instead, we compared FDG utilization in the same patient under different circumstances.

In agreement with the present results, Wahl et al. found

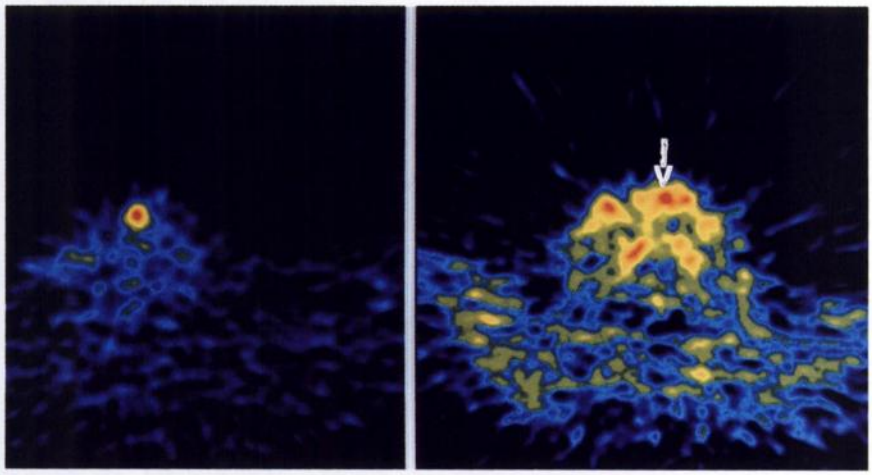

FIGURE 2. An example of PET images in the fasting state (left) and after glucose loading (right). The laryngeal tumor of Patient 5 (arrow) is clearly visible in the fasting state, but after glucose loading FDG accumulation in the tumor relative to that in the neck muscles is clearly less, making tumor visualization less distinct.

TABLE 4
FDG Uptake Calculated Using K_i Value

Patient no.	Tumor/organ, body part	K_i (min^{-1})		% Load	P-Gluc × K_i (μmol/100 g/min)		% Load
		Fast	Load	Fast	Fast	Load	Fast
1	Primary	0.049	0.029	60	26.1	30.6	117
2	Primary	0.036	0.028	79	19.2	22.6	118
3	Primary	0.067	0.042	63	39.5	52.5	133
	Metastasis	0.021	0.006	30	12.4	7.7	62
4	Primary	0.032	0.031	98	15.4	26.8	174
	Metastasis	0.021	0.029	138	10.2	24.9	244
5	Primary	0.030	0.017	57	16.7	17.4	104
	Metastasis	0.028	0.021	74	15.9	21.6	136
	Mean	0.035	0.025	75	19.4	25.5	136
1		0.057	0.025	43	30.0	25.5	85
2		0.037	0.026	72	19.7	20.9	106
3	Tongue	0.012	0.031	253	7.3	38.6	531
4	Tongue	0.012	0.026	223	5.8	22.9	396
5	Tongue	0.010	0.014	141	5.4	13.9	258
	Muscle (neck)	0.005	0.019	404	2.6	19.6	744
	Mean	0.010	0.023	255	5.3	23.7	482

* P-Gluc × K_i (=MR_{FDG} = metabolic rate for FDG).

that FDG uptake in human breast cancer cells in vitro can be inhibited by increasing the quantity of glucose in the medium. Moreover, FDG uptake appeared to have a greater decline than the increase in media glucose, suggesting saturability of the tumor uptake by excess glucose (*12*). They also demonstrated on rat mammary tumors that tumor FDG uptake dropped almost 50% at very high glucose and insulin levels, while cardiac uptake was not diminished (*13*). Similarly, Langen et al. found that FDG uptake in human lung tumors decreased in hyperglycemia (*16*).

In summary, hyperglycemia may considerably decrease FDG uptake in human tumors and impair PET image quality. Therefore, patients entering into PET-FDG studies should preferably be in the fasting state, and their blood glucose concentration needs to be taken into account. Further investigations to evaluate the influence of low blood glucose levels that occur in the fasting state on FDG tumor uptake are of importance. The effects of the blood glucose concentration on FDG uptake in different types of human cancer also needs to be investigated.

ACKNOWLEDGMENTS

We thank the personnel of the nuclear medicine department for their cooperation. This study was supported by grants from the Finnish Cancer Society.

REFERENCES

1. Warburg O. On the origin of cancer cells. *Science* 1956;123:309–314.
2. Heber D, Chlebowski RT, Ishibashi DE, Herrold JN, Block JB. Abnormalities in glucose and protein metabolism in noncachectic lung cancer patients. *Cancer Res* 1982;42:4815–4819.
3. Nolop KB, Rhodes CG, Brudin LH, et al. Glucose utilization in vivo by human pulmonary neoplasms. *Cancer* 1987;60:2682–2689.
4. DiChiro G, DeLaPaz RL, Brooks RA, et al. Glucose utilization of cerebral gliomas measured by [^{18}F]fluorodeoxyglucose and positron emission tomography. *Neurology* 1982;32:1323–1329.
5. Weber G. Enzymology of cancer cells (second of two parts). *N Engl J Med* 1977;296:541–551.
6. Gallagher BM, Fowler JS, Gutterson NI, MacGregor RR, Wan Ch-N, Wolf AP. Metabolic trapping as a principle of radiopharmaceutical design: some factors responsible for the biodistribution of [^{18}F]2-deoxy-2-fluoro-D-glucose. *J Nucl Med* 1978;19:1154–1161.
7. Som P, Atkins HL, Bandoypadhyay, D, et al. A fluorinated glucose analog, 2-fluoro-2-deoxy-D-glucose (F-18): nontoxic tracer for rapid tumor detection. *J Nucl Med* 1980;21:670–675.
8. Minn H, Joensuu H, Ahonen A, Klemi P. Fluorodeoxyglucose imaging: a method to assess the proliferative activity of human cancer in vivo. *Cancer* 1988;61:1776–1781.
9. Patronas NJ, Di Chiro G, Kufta C, et al. Prediction of survival in glioma patients by means of positron emission tomography. *J Neurosurg* 1985; 62:816–822.
10. Di Chiro G. Positron emission tomography using [^{18}]fluorodeoxyglucose in brain tumors. A powerful diagnostic and prognostic tool. *Invest Radiol* 1986;22:360–371.
11. Knuuti J, Nuutila P, Ruotsalainen U, et al. Euglycemic hyperinsulinemic clamp and oral glucose load in stimulating myocardial glucose utilization during positron emission tomography. *J Nucl Med* 1992;33:1255–1262.
12. Wahl RL, Cody RL, Hutchins GD, Mudgett E. Primary and metastatic breast carcinoma: initial clinical evaluation with PET with the radiolabeled glucose analogue 2-[F-18]-fluoro-2-deoxy-D-glucose. *Radiology* 1991;179: 765–770.
13. Wahl RL, Henry C, Ethier S. Serum glucose effects on the tumor and normal tissue uptake of FDG in rodents with breast carcinoma [Abstract]. *J Nucl Med* 1990;31:888.
14. Abe Y, Matsuzawa T, Fujiwara T, et al. Clinical assessment of therapeutic effects on cancer using ^{18}F-2-fluoro-2-deoxy-D-glucose and positron emission tomography: preliminary study of lung cancer. *Int J Radiat Oncol Biol Phys* 1990;19:1005–1010.
15. Strauss LG, Conti PS. The applications of PET in clinical oncology. *J Nucl Med* 1991;32:623–648.
16. Langen K-J, Braun U, Rota Kops E, et al. The influence of the plasma glucose level on ^{18}F-deoxyglucose uptake in human pulmonary neoplasms [Abstract]. *2nd European Workshop on FDG in Oncology.* Heidelberg, 1991.
17. Okada J, Yoshikawa K, Itami M, et al. Positron emission tomography using fluorine-18-fluorodeoxyglucose in malignant lymphoma: a comparison with proliferative activity. *J Nucl Med* 1992;33:325–329.
18. Griffeth LK, Dehdashti F, McGuire AH, et al. PET evaluation of soft-tissue masses with fluorine-18 fluoro-2-deoxy-D-glucose. *Radiology* 1992; 182:185–194.23.

19. Leskinen-Kallio S, Ruotsalainen U, Någren K, Teräs M, Joensuu H. Uptake of carbon-11-methionine and fluorodeoxyglucose in non-Hodgkin's lymphoma: a PET study. *J Nucl Med* 1991;32:1211–1218.
20. Kern KA, Brunetti A, Norton JA, et al. Metabolic imaging of human extremity musculoskeletal tumors by PET. *J Nucl Med* 1988;29:181–186.
21. Haberkorn U, Strauss LG, Reisser CH, et al. Glucose uptake, perfusion, and cell proliferation in head and neck tumors: relation of positron emission tomography to flow cytometry. *J Nucl Med* 1991;32:1548–1555.
22. Olefsky JM. Obesity. In: Wilson JD, Braunwald E, Isselbacher KJ, eds. *Harrison's principles of internal medicine, volume 1*, 12th edition. New York: McGraw-Hill; 1991:411.
23. UICC. International union against cancer. *TNM classification of malignant tumours*, 4th edition. Geneva: 1987.
24. Hamacher K, Coenen HH, Stöcklin G. Efficient stereospecific synthesis of no-carrier-added 2-[^{18}F]-Fluoro-2-Deoxy-D-Glucose using aminopolyether supported nucleophilic substitution. *J Nucl Med* 1986;27:235–238.
25. Patlak CS, Blasberg RG, Fenstermacher JD. Graphical evaluation of blood-to-brain transfer constants from multiple-time uptake data. *J Cereb Blood Flow Metab* 1983;3:1–7.
26. Reivich M, Alavi A, Wolf A, et al. Glucose metabolic rate kinetic model parameter determination in humans: the lumped constants and rate constants for [^{18}F]fluorodeoxyglucose and [^{11}C]deoxyglucose. *J Cereb Blood Flow Metab* 1985;5:179–192.
27. Fidler I. The biology of human cancer metastasis. *Acta Oncol* 1991;6: 669–675.
28. Herholz K, Ziffling P, Staffen W, et al. Uncoupling of hexose transport and phosphorylation in human gliomas demonstrated by PET. *Eur J Cancer Clin Oncol* 1988;7:1139–1150.
29. Lammertsma AA, Brooks DJ, Frackowiak RSJ, et al. Measurement of glucose utilization with [^{18}F]2-fluoro-2-deoxy-D-glucose: a comparison of different analytical methods. *J Cereb Blood Flow Metab* 1987;7:161–172.
30. Herholz K, Wienhard K, Heiss W-D. Validity of PET studies in brain tumors. *Cereb Brain Metab Rev* 1990;2:240–265.
31. Spence AM, Graham MM, Munzi M, et al. Assessment of glucose metabolism in malignant gliomas: use of deoxyglucose or glucose [Abstract]. *Second European Workshop on FDG in Oncology*. Heidelberg, 1991.

EDITORIAL

FDG-PET in Oncology: There's More to It Than Looking at Pictures

"Things sweet to taste may prove in digestion sour."
William Shakespeare

Rapidly proliferating tumor cells metabolize glucose more rapidly under anerobic than under aerobic conditions. This inhibition of glycolysis by oxygen, the "Pasteur effect," was first described by Pasteur and later confirmed by Warburg and Meyerhof (*1,2*). Proposed explanations for this phenomenon include, increased concentrations of hexokinase in tumors compared to normal tissue and increased glucose transport into tumors (*3–5*). Accelerated glucose transport is among the most characteristic biochemical changes that occur with cellular transformation. In a recent study, the molecular mechanism of altered glucose transporter activity was evaluated in cultured rat fibroblasts transfected with activated myc, ras and src oncogenes (*6,7*). In cells transfected with myc, the rate of 2-deoxy-D-glucose transport was unchanged. In contrast, transfection with ras and src oncogenes resulted in dramatically increased glucose transport which was paralleled by marked increases in the amounts of glucose transporter protein and messenger RNA. Similarly, exposure of the cells to the tumor promoting phorbol ester 12-O-tetradecanoyl phorbol-13-acetate also resulted in accelerated glucose transport and increased concentrations of transporter mRNA. These results indicate that a significant mechanism by which malignant transformation activates glucose transport is increased expression of the structural gene encoding the glucose transport protein.

The ex vivo evaluation of glucose metabolism in tumors can be performed with ^{3}H or ^{14}C-labeled glucose. However, the fact that glucose is extensively metabolized in vivo requires detailed chromatographic analysis of the concentration of individual metabolites. The introduction of radiolabeled 2-deoxy-D-glucose by Sokoloff et al. as a tracer of glucose metabolism has greatly facilitated these measurements (*8*). Since this tracer lacks a hydroxyl group in the 2 position, the first glucose metabolite, 2-deoxy-D-glucose-6-PO_4, is not a substrate for glucose-phosphate isomerase and cannot be converted to fructose-6-PO_4. For similar reasons, 2-deoxy-D-glucose cannot be converted to glycogen. Thus, the formation of 2-deoxy-D-glucose-6-PO_4, is the final step in the absence of glucose-6-phosphatase, which catalyzes the reverse reaction to 2-deoxy-D-glucose. Since it is highly negatively charged, 2-deoxy-D-glucose-6-PO_4 accumulates intracellularly. Due to the isoteric relationship between hydrogen and fluorine, the positron emitting glucose analog 2-[^{18}F]fluoro-2-deoxy-D-glucose (FDG) can be used for the in vivo measurement of glucose metabolism in humans by PET.

Following injection, FDG is transported into the cells of most tissues by facilitated diffusion, phosphorylated to FDG-6-PO_4 and trapped intracellularly (*8–11*). Thus, the annihilation photons of ^{18}F that are detected by PET originate from FDG in plasma and tissue and intracellular FDG-6-PO_4. Within 1 hr after injection, most of the radiation emitted from tissues with low concentrations of glucose-6-phosphatase, such as heart, brain and many tumors, comes from intracellular FDG-6-PO_4. Tissues with high levels of this enzyme, such as liver, kidney, intestine and muscle, accumulate small amounts of FDG-6-PO_4 and contribute a low level of background radioactivity to PET images.

Received Sept. 21, 1992; accepted Sept. 21, 1992.

For correspondence or reprints contact: Dr. Alan J. Fischman, Division of Nuclear Medicine, Department of Radiology, Massachusetts General Hospital, 32 Fruit St., Boston, MA 02114.